

Visuohaptic Borescope Inspection Simulation Training: Modeling Multi-Point Collision Detection/Response and Evaluating Skills Transfer

Deepak Vembar, Andrew Duchowski*
School of Computing
Clemson University

Melissa Paul, Anand Gramopadhye
Industrial Engineering
Clemson University

Carl Washburn
Aircraft Maintenance Program
Greenville Technical College



Figure 1: Visual comparison of intersection response of actual and virtual probe at 30° angle of incidence (for visualization purposes only—the user's viewpoint is from the probe's tip); inspection of PT-6 aircraft engine using actual borescope, with operator's view of the camera output.

ABSTRACT

Results are presented from a transfer effects study of a visuohaptic borescope simulator developed for non-destructive aircraft inspection training. The borescope simulator supports multi-point collision detection to effect haptic feedback as the virtual probe slides along and collides with rigid surfaces. Such probe maneuvering is shown to be a significant aspect of the inspection task that benefits from training, regardless of whether a real or virtual probe simulator is used to provide the training.

Index Terms: I.3.6 [Computer Graphics]: Methodology and Techniques—Ergonomics; J.4 [Computer Applications]: Social and Behavioral Sciences—Psychology.

1 INTRODUCTION

In aircraft maintenance, visual inspection forms an important part of non-destructive testing [2] accounting for almost 80% of planned maintenance of large aircraft [7]. Due to minimal equipment costs, visual inspection is usually the quickest and most economical way of obtaining a preliminary evaluation of the condition of an aircraft [6]. Inspection of easily accessible regions of an aircraft such as cargo bay and fuselage require simple equipment, such as a flashlight and magnifying glass. Enclosed components, such as an aircraft engine, present a challenge as the parts are not easily accessible without a complete teardown of the equipment.

To enable a technician to inspect an area that is inaccessible by other means, a device known as a borescope is used. A borescope is an optical device consisting of a rigid or flexible tube with an eyepiece or video screen at one end and a miniaturized camera or lens system at the other end. The two components are linked together by a fiber optic cable which carries a video signal and serves to illuminate the engine component under inspection.

Theoretical knowledge of borescope inspection is generally gained in the classroom. On-the-job training by a more experi-

enced inspector is used to bridge the gap from an academic setting to a more practical workplace environment. However, this transition from the classroom to the workplace is not easy. Many novice inspectors face a steep learning curve because they lack the required hands-on experience required to make a smooth transition to the workplace. The major limitation in providing more practical experience to students is the prohibitive cost associated with obtaining different types of aircraft to train the students.

Virtual Reality (VR) simulators have been used to train novices in a wide range of skills, including flight and surgery [3, 16]. Consisting of 3D models rendered by a computer, simulators attempt to present a realistic, real-time environment with instantaneous performance feedback. Training sessions can be customized to suit individual needs and skill levels. In addition to purely visual feedback, simulators can be augmented with auditory and tactile feedback for a more immersive experience. It is hypothesized that *functional realism* [15] of the VR simulation is necessary for the skills to transfer effectively from the virtual testbed to the real world.

Earlier, we described a novel virtual borescope inspection simulator [29]. Using 3D models of engine components, we developed the simulator to train novice borescope inspection technicians in the good practices of engine inspection. User interaction was tested with a novel haptic device as well as with off-the-shelf devices such as the Novint Falcon. By providing probe tip contact feedback and a realistic probe camera model, we established the benefit of force feedback by observing improved task completion times as well as reduced probe intersections in the simulator. However, some participants noted they did not receive any force feedback from the haptic device when inserting and maneuvering the virtual probe through the engine model.

Presently, a mathematical model for multi-point collision detection and response along the length of the virtual probe is derived. Previously, multiple points of contact were detected, but force feedback was calculated only at the tip of the probe. As visualized in Figure 1, computation of forces along the probe's length allows provision of sliding contact feedback to the user as the probe grazes surfaces in the virtual environment. The sliding contact feedback, augmenting tip contact feedback, is thought to further decrease performance uncertainty by affording the user with a richer compar-

*e-mail: duchowski@clemson.edu

ison to expected kinesthetic sensations, and thus hypothesized to reduce *functional task difficulty* [17]. We do not test this hypothesis directly, however.

While sliding contact is tacitly assumed to enrich haptic feedback, in this paper we focus on the evaluation of training transfer effects on real world task performance. Prior evaluation of the borescope simulator was limited to representative inspection tasks in the simulator. We did not perform any evaluation of task performance during an actual engine inspection. Here, quantitative and qualitative measures are reported from novice students inspecting a PT6 engine after undergoing one of three training methods: classroom-only training, simulator training, or hands-on training with the video borescope. Results indicate that the psychomotor skills required for maneuvering the borescope probe through the engine can be successfully obtained through simulator training.

2 PHYSICALLY-BASED PROBE MODEL

While graphics rendering focuses on the visual appearance of the model, by computing appropriate force/torque interaction, haptic rendering simulates force feedback to allow the human operator to feel the geometry, surface, and material properties of the object. There are two major points of asymmetry between haptic and graphics rendering: collision detection and rate of dynamic simulation. Unlike graphics rendering which only needs to model object deformation to “look” realistic, haptic rendering has to be built upon a more accurate physics-based model. While real-time update rates for graphics rendering are about 30-60 frames per second, smooth haptic rendering requires an update rate of almost 1 KHz.

In haptic interface design, the deciding factor in choosing the best collision algorithm is the speed of calculation to determine whether a collision has occurred. Inter and intra-object collisions play an important role in the overall behavior of the interacting objects in a simulation. The choice of the contact model, single point versus multi-point contact detection, and external forces such as static and dynamic friction, influence the post-impact motion of the interacting objects. Quick changes in haptic forces when objects intersect can cause artificial growth of energy and lead to instabilities of the simulation [27].

2.1 Prior work

Prior work in the medical simulation community has led to the development of fast, scalable, multi-object, multi-point collision simulation and response algorithms [4]. Intersections of the borescope probe with the engine can occur at multiple points along the inserted length. Probe deformations occur due to collisions with the engine, and the amount of deformation is dependent on the position within the engine, force applied at the point of incidence, as well as the angle of incidence of the probe at the point of contact. Unlike medical procedures, which use a catheter, such as in vascular and cardio-thoracic surgery, interaction of the borescope probe with the engine consists of a semi-flexible body interacting with a rigid body. Instead of computing elastic and deformation forces experienced by the catheter due to collision with soft tissues, computation of deformations can be limited to the interaction of the semi-flexible probe with rigid surfaces.

Prior work, especially in radiology and vascular surgery [5, 24], has resulted in visual and behaviorally realistic models for simulating catheters, guidewires and surgical threads. Deformable objects have been simulated using physically-based mass-spring models following Newtonian Laws of motion. The catheter or surgical thread is modeled as a linear system of point masses connected by linear and torsional springs between two adjacent points. Using explicit or implicit numerical integration, the velocities and positions of each point mass are computed over the duration of the simulation. Since collision detection is computationally expensive, methods such as bounding spheres, axis-aligned bounding

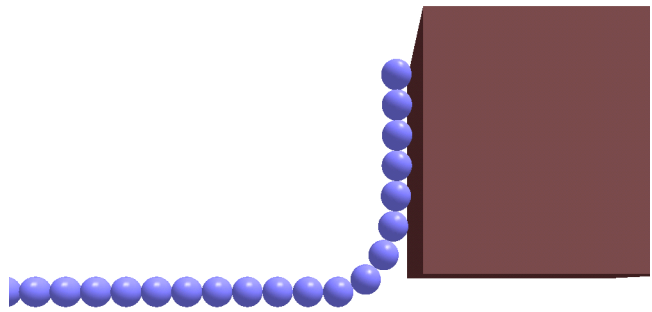


Figure 2: Visualization of node chain used to model the borescope.

boxes (AABBs) or bounding volume hierarchies (BVHs) are used to speedup collision testing.

The main advantage of mass-spring models is that they are fast, easy to implement and, with appropriate collision detection algorithms, can support haptic rates exceeding 1 KHz. Several previous examples exist, including Dawson et al.’s [12] catheter simulation based on a multi-body system composed of a set of rigid bodies and joints, Pai’s [25] one-dimensional deformable objects modeled as Cosserat rods, Brown et al.’s [8] physical simulation model called Follow The Leader (FTL), Alderliesten et al.’s [1] simulation of guidewire insertion into the vascular system, Wang et al.’s [30, 31] physics-based simulation of a thread model, and Kubiak et al.’s [18] real-time simulation of thread dynamics with all the relevant aspects of the physics model of the thread, including stiffness, bending, torsion and self-collision, and output forces for haptic feedback. The stability of these systems depends to a great extent on the simulation parameters chosen. Simulation of interactions of rigid objects with large stiffness requires a small timestep for numerical stability, which in turn affects the interactive rate of the simulation. Biological materials, such as tissues, exhibit non-linear elasticity and are not at all homogeneous, so choosing realistic simulation parameters for the spring constants is time consuming.

In mass-spring systems, the object is represented as a set of discrete point masses connected by springs. The initial formulation is discrete and any deformations of the model changes the level of potential energy in the model. Finite Element Models (FEMs), on the other hand, have been proposed as a solution to the difficulties with simplified physically-based systems. FEMs provide a continuous formulation that relates the model deformation to energy and compute deformation over the entire volume instead of at discrete points. They are more accurate than mass-spring systems, but at the expense of added computational complexity. Examples include those of Contin et al. [11], who developed a real-time model for deformation of devices such as catheters and guidewires during navigation inside complex vascular networks, and Lenoir et al. [22], who used a composite model to realistically simulate a catheter/guidewire system,

In addition to the graphical simulation of deformable objects, Laycock and Day [20, 21] have presented multiple algorithms to model the interactions of a deformable tool with a rigid body. The deformable tool, in this case an elastic rod, is modeled as a linear chain of 6-DOF nodes and its behavior is calculated using FEM analysis. Translational and rotational properties as well as realistic deformation of the beam elements were implemented. However, the simulation performance degraded as the number of nodes increased, due to the computational complexity of increased collision detection required for the additional nodes.

Our implemented probe model (Figure 2) is based on Globular Elastic Models (GEMs) [10] used to simulate deformable objects, but instead of computing the medial axis transform, the borescope

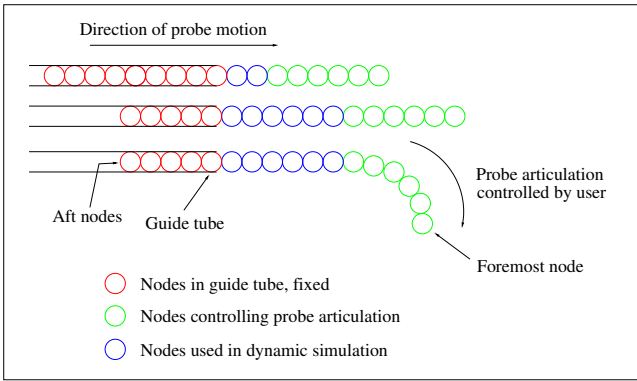


Figure 3: Representation of the linear chain of nodes used to model the borescope probe. Each adjacent pair of nodes is connected by a set of linear and angular springs.

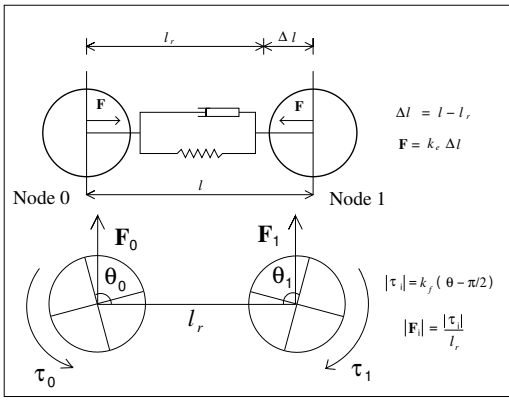


Figure 4: Elongation and torsion due to linear and angular springs between two adjacent nodes of the probe.

probe is modeled as a discrete linear chain of point mass nodes (p_0, \dots, p_n) with damped linear and angular springs connecting adjacent nodes. We implemented a simple numerical integrator using Euler’s method, as opposed to using middleware APIs such as Havok Physics or the Open Dynamics Engine (ODE). We describe the model in the following section.

2.2 Implementation

Successful implementation of a physically based probe model requires fast detection of collisions, computation of interacting forces from an internal mass-spring model of the simulation as well as external forces due to the point-proxy model, and collision response from the computed forces. We implemented a hybrid probe model combining the deformation modeling of a linear mass-spring system, and collision detection and response through a chain of point-proxy nodes.

2.2.1 Conceptual Model

Figure 3 shows a diagrammatic representation of the borescope probe model. The foremost nodes control articulation of the virtual probe. Rotational torques can be directly applied to the foremost node, which is used to calculate the final position of the trailing nodes in the model through dynamic simulation of the whole mass-spring system. The nodes abaft the lead nodes do not directly control the articulation of the tip, but simulate the connected linear length of the probe. Aft nodes in the guide tube serve as anchor nodes and do not take part in the control of the tip articulation.

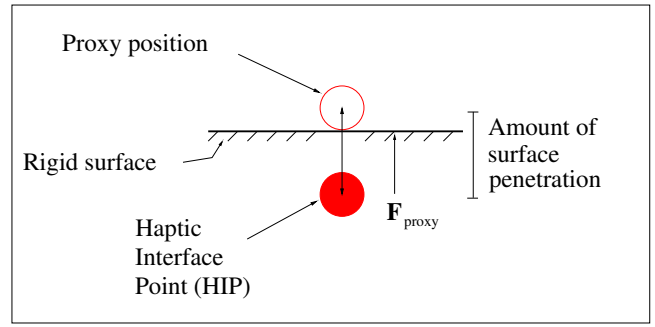


Figure 5: Single point contact with position of Haptic Interface Point (HIP) and proxy position.

Linear elongation springs between adjacent nodes provide axial compression and elongation, and angular springs simulate flexion and torsion of the probe. The behavior of linear and angular springs is based on Hooke’s Law. The rest length between two adjacent nodes, l_r , is a predefined constant (see top of Figure 4). To simulate bending curvature, the rest length between the adjacent nodes should be small. The linear elongation and compression forces experienced by the nodes connected by an axial spring are given by $\mathbf{F} = -k_e \Delta l$, where \mathbf{F} is the restoring force exerted by the spring, k_e is the spring linear constant, and $\Delta l = l - l_r$ is the amount of elongation or compression from rest length, l_r .

Similarly, the angular torques experienced by the probe due to flexion about the y and z -axes (see bottom of Figure 4) cause articulation of the probe. Four angular springs are used to control the orientation of the nodes about the center line. Torques due to flexion are computed as $\tau = -k_f \Delta \theta$ where τ is the computed angular torque due to flexion, k_f is the angular spring constant, and $\Delta \theta$ is the change in the angular orientation from its rest orientation. Torsion, or twisting of the probe about the longitudinal axis, is due to a single angular spring between two adjacent nodes. It is computed similar to flexion and applied to both nodes.

Although the parameters of the spring constants are important, prior work has used heuristic methods to determine these values. In our case, axial compression and torsion about the longitudinal axis (x -axis) is significantly smaller compared to the flexion about the y and z -axes. This was modeled by using large values of spring constants for elongation and torsion, but smaller values for flexion.

In addition to computing the internal forces due to elongation, flexion and torsion of the springs connecting the nodes, damping forces were also computed and applied to stabilize the mass-spring system and to prevent oscillations. The system was critically damped, with the damping constant computed for each spring as: $\mathbf{d} = 2\sqrt{km}$ where \mathbf{d} is the computed damping constant, k is the spring constant, and m is the mass of the node. Damping forces were computed for each of the three springs acting on the node. Unlike computing the forces on a per-node basis, the damping forces were computed on a per-link basis, and applied to each of the nodes connected to the springs, but in opposite direction to the application of the spring forces.

2.2.2 Collision Detection and Response

Haptic rendering is the process of computing a reaction force for a given position of the haptic interface in the virtual world. Unlike visual stimulus, human estimation of spatial dimensions through haptic exploration has a larger threshold for error. In single point haptic interaction, the haptic device allows the user to interact with the objects in the virtual world. To prevent the Haptic Interface Point (HIP) from penetrating into the objects, Zilles et al. [33] proposed the “God-object” and Ruspini et al. [26] the “virtual proxy”

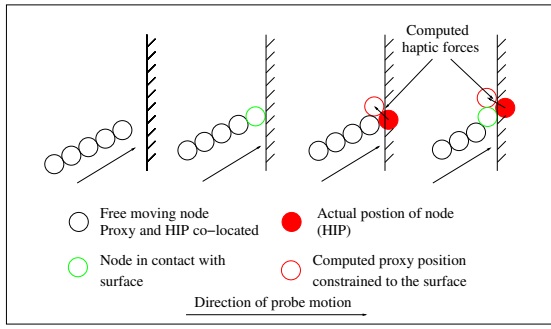


Figure 6: Simulating multiple points of contact, taking into account dynamics of the mass-spring system and point-proxy HIP forces.

models, where the visual representation of the HIP in the scene, the proxy, is constrained to the surface of the object it is in contact with, as opposed to penetrating the object (see Figure 5). The proxy point is constrained to lie on the surface of the object, and represents the position of the HIP in the scene if the object were infinitely stiff.

The contact point of the HIP and objects in the scene can be obtained through simple geometric methods and the proxy-point force algorithm used to compute the haptic interaction forces. The most commonly used function to compute the feedback force is based on the penalty method, where the force exerted due to penetration of the HIP into the model is $\mathbf{F} = -k\delta$, where \mathbf{F} , the reaction force, is computed as a function of k , the spring constant (usually a large number for stiff objects), and δ is the linear distance between the HIP and the proxy point.

We extended the single point-proxy method to multiple contact points to model the interaction of the borescope probe. In addition to the linear chain of point masses as described earlier, each node is associated with a proxy node. The proxy node is used for probe visualization by constraining its position to the surface of the intersecting object. The proxy node also serves to exert an unbalanced external force based on the penalty method, which is applied to the node as an external force and used in the position calculation.

Figure 6 depicts the interaction of the simulated probe consisting of 5 nodes colliding with a rigid wall. The arrow at the bottom of the figure depicts the direction of motion of the probe. In the left panel of the figure, the probe is free to move and there is no intersection with the wall. On detecting intersection (middle panel), at the point of contact, both the actual and the proxy position of the node are co-located. As long as there is no further motion of the probe, the force exerted at the contact proxy position is zero. In the right-most panel, the probe has advanced further along the direction of motion. The actual position of the leading node is inside the wall, but the computed position of the proxy node (depicted as a colored circle) is constrained to the surface of the object. External forces computed by the proxy-point algorithm are added to the position of the node (filled circle) and the dynamic simulation of the probe computed. As long as the actual and the proxy position of the node are different, a linear spring force is exerted.

2.2.3 Multi-Contact Force Feedback

In prior versions of the simulator [29], force feedback was limited to direct contact of the tip of the virtual borescope with the engine models. Although direct force feedback is important in preventing damage to the tip of the real borescope, experienced inspectors also rely on the feedback obtained from intersections of the engine along the length of the probe. This feedback, though not as direct as tip feedback, helps the technician guide the borescope through the engine. Representing multiple points of contact in the virtual borescope simulator using a haptic interface such as Novint's Fal-

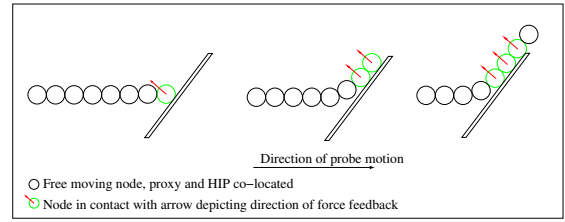


Figure 7: Computation of forces for multiple points of contact.

con is challenging, as the device provides only a single resultant force, effectively simulating a single point of contact.

To simulate feedback from multiple points of contact using the haptic interface, we developed a simple algorithm that computes the resultant force based on the total number of nodes of the virtual probe in contact with the 3D model of the engine. There are three common cases when the virtual probe interacts with a surface as shown in Figure 7 that have to be considered when developing the algorithm to determine the resultant force.

In the first case, consider the interaction of the probe with the surface (leftmost panel). The foremost node of the probe is in contact with the surface. With a single node in contact, the force feedback is limited to a single force acting on the node as shown in the figure. The force and the direction of action of the force can be represented easily with a 3-DOF force feedback device such as the Falcon.

In the second case, both the foremost node and the nodes abaft are in contact with the surface (middle panel in Figure 7). The collision detection algorithm and the proxy nodes constrain the nodes along the surface. When the virtual probe moves from the left to the right towards the surface, more nodes of the virtual probe come into contact with the surface. Representation of the force feedback by the haptic device has to now take into consideration the force feedback on the leading node as well as the feedback on the node adjacent to it that is in contact with the surface.

Finally, consider the last panel in Figure 7. The leading node has progressed beyond the edge of the surface and is no longer in contact with the surface. However, probe nodes abaft the leading node are still in contact with the surface. The force algorithm has to take into consideration the resultant force of all the nodes in contact with the surface, as well as compute the resultant direction of application of the force.

To compute the resultant single force to be rendered by the haptic device, a linear combination of all the forces experienced by the virtual probe is calculated. The total force is computed as the force experienced by the foremost node and the clamped linear sum of the other nodes in contact with the engine model. Assuming n nodes of the borescope are in contact with the surface, the total force \mathbf{F}_{total} is calculated as:

$$\mathbf{F}_{total} = \mathbf{F}_{tip} + \max(0, \min(\mathbf{F}_{max}, \sum_{i=0}^n \mathbf{F}_i)),$$

where \mathbf{F}_{tip} is the total force experienced by the tip node, \mathbf{F}_i is the force experienced by the i^{th} node in contact with the surface, and \mathbf{F}_{max} is maximum contribution towards the total force.

The Novint Falcon has a maximum continuous force output of 2 lbs or 8 N. The contribution of the total force \mathbf{F}_{total} was thus limited to 8 N, with the contribution of foremost node clamped at 6 N and the contribution of the other nodes clamped at 2 N.

2.2.4 Numerical Integration

In the simulation of the probe, we had to consider the interaction of the user with the borescope probe. There are two basic actions that the user performs during borescope inspection: insertion of

the probe into the engine, and tip articulation using the hand-held interface. We simulated the virtual probe as it emerges from the guide tube in the virtual model of the engine. A gamepad is used to directly control the articulation of the virtual probe by applying an unbalanced torque to the foremost node of the probe tip. Simulation of the probe takes into consideration both the internal forces acting on the nodes due to the mass-spring system as well as the external forces that arise due to node contact with objects in the scene.

The dynamic simulation consist of the following steps.

1. Clear internal forces and torques. At the beginning of the simulation, each node starts at equilibrium where there are no internal unbalanced forces. There may be external forces such as the contact forces that arise from the probe proxy as it collides with the models in the environment or external unbalanced articulating torques applied to the foremost node of the virtual probe.
2. Calculate per-node and per-link forces and torques. The internal forces due to elongation, flexion and torsion springs used to connect the adjacent nodes in the mass spring system are computed at each step in the simulation and stored in the state space of the nodes they affect.
3. Integrate. Calculated forces and torques are used to compute the next position and orientation of the lead node via explicit numerical integration. As we used a large number of nodes (100 nodes and proxy nodes) for collision detection and response, we used Euler integration as opposed to 4th-order Runge-Kutta to reduce the computational overhead and maintain the haptic thread at 1 KHz.
4. Render. The lead node's position and orientation are updated and it is checked for collision with the virtual objects in the scene to prevent interpenetration.

Simple Newtonian motion can be represented by the equations $\mathbf{F} = m\ddot{\mathbf{x}}$ and $\boldsymbol{\tau} = m\alpha$, where \mathbf{F} and $\boldsymbol{\tau}$ are the sum total of all the forces and torques acting on the node and m is the mass of the node. In our simulation, each node in the probe is expressed as a state vector, $[\mathbf{x}, \dot{\mathbf{x}}, \ddot{\mathbf{x}}, \theta, \omega, \alpha]$, where the terms $(\mathbf{x}, \dot{\mathbf{x}}, \ddot{\mathbf{x}})$ represent position, velocity, and linear acceleration, while (θ, ω, α) represent orientation, angular velocity, and angular acceleration, respectively. Assuming that the forces and the torques acting on a node can be calculated at the beginning of the timestep $n + 1$, we can compute the instantaneous linear and angular acceleration as $\ddot{\mathbf{x}}_{n+1} = \mathbf{F}/m$, and $\alpha_{n+1} = \boldsymbol{\tau}/m$, respectively. The velocities and position/orientation at timestep $n + 1$ can be computed through simple numerical integration of the ordinary differential equations:

$$\begin{aligned} \mathbf{x}_{n+1} &= \mathbf{x}_n + \dot{\mathbf{x}}_{n+1}\Delta t, & \theta_{n+1} &= \theta_n + \omega_{n+1}\Delta t \\ \dot{\mathbf{x}}_{n+1} &= \dot{\mathbf{x}}_n + \ddot{\mathbf{x}}_{n+1}\Delta t, & \omega_{n+1} &= \omega_n + \alpha_{n+1}\Delta t \end{aligned}$$

The position and orientation of a node at timestep $n + 1$ is stored and used to compute the proxy positions of the node at timestep $n + 2$ by checking for collision with the virtual objects in the scene.

3 REAL-WORLD TASK PERFORMANCE

The borescope is similar in design to commonly used medical tools such as the endoscope. Both instruments are used to check for abnormalities by visual inspection. The skills and the hand-eye coordination needed to manipulate the articulating tip in both these devices are similar in nature. Past research has led to the development of desktop VR simulators for training doctors in bronchoscopy, colonoscopy, mastoidectomy, etc. [12, 14, 19]. Virtual endoscopy consists of navigation of a virtual camera through a 3D reconstruction of a patient's anatomy enabling diagnosis or the exploration of the internal structures to assist in surgical planning [23].

Evaluation studies used to assess the realism of such simulators showed that participants felt that the virtual simulators strongly represented the real world environment. Ferlitsch et al. [13] observed that novices trained on such simulators performed their tasks faster and with fewer errors than those who did not have similar training. They also observed that there are distinct differences between the strategies adopted by expert doctors and novices when they were asked to use the simulator. It was also found that using real life props, such as a mannequin, and providing real time force feedback increased the sense of presence and realism of the virtual simulator [28]. Lamata et al. [19] attempted to provide baseline metrics for incorporating virtual simulators in training doctors in laparoscopy using virtual trainers. Although repeated training on the simulators has been found to improve the performance of novices, the transfer effects of training on virtual simulators and performance in the real world are not fully understood.

One of the primary goals of the borescope simulator was to enhance classroom instruction by providing hands-on training in a replicated simulation of the inspection task. Prior evaluations of the virtual borescope to determine the visual control and haptic fidelity of the simulator were restricted to evaluation of pre- and post-training metrics on the simulator. While literature evaluating the effectiveness of simulator training suggests a trend of simulator performance being a good predictor of real world performance, we wanted to determine if simulator training would be comparable to real world training with the actual device.

We evaluated three different training methods: classroom-only training, borescope simulator training with force feedback, and hands-on training with the real video borescope. We were interested in comparing classroom-only instruction, emphasizing theoretical knowledge, with hands-on learning through repeated practice on the virtual borescope simulator. In addition, we wanted to determine if the skills required for successful engine inspection could be successfully obtained through simulator training.

3.1 Participants

Twenty six students enrolled in the aircraft maintenance program at Greenville Technical college took part in this study. All the students had completed at least two semesters of general aviation inspection related coursework and were familiar with the theoretical background on engine inspection. Participants had limited hands-on experience with the video borescope having observed its use by the classroom instructor. A few of the participants had limited experience with an optical borescope.

Students were divided into three groups; one group with eight participants and the other two groups with nine participants each. Training (the independent variable) varied across groups.

1. Control group. Participants in this group received no hands-on training other than theoretical knowledge through classroom instruction.
2. Virtual borescope (simulator) group. Participants in this group received two 45-minute training sessions on the virtual borescope simulator, followed by a 10-minute evaluation with the simulator to determine their proficiency with user controls and inspection procedures.
3. Video borescope (hands-on training) group. Participants received two 45-minute training sessions through hands-on operation of a real video borescope on an aircraft engine.

3.2 Apparatus and Stimuli

Students in the simulator group received inspection training on the virtual borescope simulator. The simulator was run on a desktop PC, equipped with a PentiumD 2.4GHz processor, 4GB RAM, and a GeForce 9800GT video card. The output of the simulator was

presented on a 19" LCD monitor placed in front of the participant in a 1024×768 window. The visual stimulus provided to participants consisted of a polygonal model of the PT-6 engine, modeled and textured in Maya. The rendering of the engine components and the haptic feedback calculations was handled by CHAI libraries [9], an open-source API for graphical and haptic rendering. The probe model implemented allowed the user to rotate the virtual camera in a hemisphere about the probe's axis. Camera articulation of the virtual probe was controlled by an off-the-shelf gamepad. An off-the-shelf Novint Falcon was used both for controlling the amount of virtual probe insertion into the 3D engine as well as to provide force feedback of the contact forces experienced by the virtual probe.

The students in the hands-on training group received inspection training using the Olympus video borescope. A representative engine of a PT6 aircraft was dismantled to expose the hot section components consisting of the stator and rotor, as shown in Figure 1. A guide tube was inserted into the fuel injection manifold at the top of the engine casing to allow easy insertion of the borescope into the engine and facilitate inspection of the rotor. An experienced borescope inspector was present to provide instruction and guidance on the best practices while inspecting with the borescope.

3.3 Procedure

At the beginning of the experiment, the participants filled out a demographic questionnaire on their experience with training simulators and the video borescope. The experiment was carried out over three days to prevent fatigue and avoid influencing the results of the experimental evaluation.

On day 1, the control group received no training on the simulator or the actual engine. The simulator group was provided training with the virtual borescope, with a focus on familiarizing the participants with the articulation and insertion controls of the simulator. Participants were first introduced to the simulator and the use of the gamepad and the Falcon to control the virtual probe. Next, participants spent approximately 45 minutes interacting with the simulator and getting used to the articulation controls. In addition to psychomotor skills training, we also provided good practices inspection training by having the participants inspect the engine model in a systematic fashion. Numbered textures on the engine model emphasized this aspect of training, with arrows prompting successive stages of inspection. At the end of the familiarization phase, participants were tested on their progress by performing a simulated task of inspecting 15 rotor blades for defects. Quantitative measures of time to complete the task and the total number of probe tip intersections with the engine model were collected for offline analysis.

The training provided to the borescope training group consisted of introduction to the video borescope, a brief summary of controlling the probe tip with the articulation joystick and good practices in borescope inspection. On completion of these steps, the participants used the borescope and performed a 45 minute inspection on a PT-6 engine. The engine was pristine and did not have any defects, as we wanted the participants to become accustomed to the interface as opposed to the task of defect detection.

On day 2, the steps followed were similar to day 1 for all three groups with a few minor changes. In addition to providing good practices inspection for the simulator group, they were also provided training to detect common defects such as cracks and corrosion in the engine. Defect textures were developed and mapped on the engine model to provide a brief overview of different engine defects. At the end of the simulator training, quantitative data was collected to compare the influence (if any) of longer training durations on participants' performance over the two days. There were no changes to the training provided to the other two groups.

On day 3, all three groups were tested on a PT-6 engine using the video borescope. The engine used in this study differed from the one used for training the hands-on group in order to reduce learn-

ing effects. Random blades were painted with a white X simulating rotor defects (recall we are focusing on probe usage training, not on inspection search and decision making). As the control and simulator groups were using the video borescope for the first time, they were provided a 10 minute introduction to the video borescope and its articulation controls.

The inspection process consisted of participants inserting the borescope probe into the engine through the guide tube and maneuvering the borescope probe through the engine stators to obtain a good view of the rotor. Once the participant had a clear view of the leading edge and the base of the rotor blades, the inspection task consisted of looking for the painted markers on the blades. An accomplice manually rotated the engine to turn the rotor so that the participant could concentrate on borescope probe manipulation and controlling the camera articulation along with defect detection. Once the participant completed inspecting all 58 blades of the rotor, they were instructed to complete the inspection task by withdrawing the probe from the engine.

3.4 Experimental Design and Data Collected

A between-subjects completely random experimental design was used to study the transfer effects of simulator training. The 26 participants were randomly assigned to one of the three training groups. Training condition served as the independent variable. Performance data collected was time taken to complete the task, broken down into 4 intervals: (1) inserting the borescope probe through the guide tube into the engine, (2) maneuvering the probe through the stator to obtain a clear view of the rotor blades for inspection, (3) systematically inspecting the blades for simulated defects, and (4) withdrawing the borescope probe from the engine.

The control group was expected to yield the the largest mean inspection times, compared to the simulator and hands-on training groups. The simulator and borescope training groups were expected to achieve similar performance due to improved skill levels compared to classroom-only training group.

The virtual borescope group had additional performance and subjective data collected at the end of each individual training sessions. The total time to complete the simulator inspection and the number of intersections of the virtual camera with the engine model were collected and analyzed to determine the effects of repeated training on task performance in the simulator. On completion of the training, the participants filled out a modified Witmer-Singer Presence Questionnaire [32], with responses to the questionnaire on a 7-point Likert scale, with 1 being most negative, 4 neutral, and 7 most positive.

It was hypothesized that due to longer training, total inspection time and number of intersections with the engine model would decrease from day 1 to day 2.

3.5 Results

Figure 8 shows the mean completion times for all three training conditions, as well as the breakdown of the time taken to perform each of the four phases of the inspection task identified in the previous section. ANOVA of the mean completion times shows that there were significant differences among the three groups ($F(2,23) = 40.3$, $p < 0.01$), with the control group taking longer to complete the inspection task compared to the other two groups who received training. Pairwise t-tests (with Bonferroni correction) reveal no significant difference between the virtual borescope and real borescope group. However, there were significant differences in time to completion between the control group and the two training conditions ($p < 0.01$ for both pairings).

The Kruskal-Wallis test was used to analyze the time taken for each individual stage of the inspection, as Shapiro-Wilk's test revealed non-normal data distribution. There was no significant difference among the three groups for the average time taken to insert

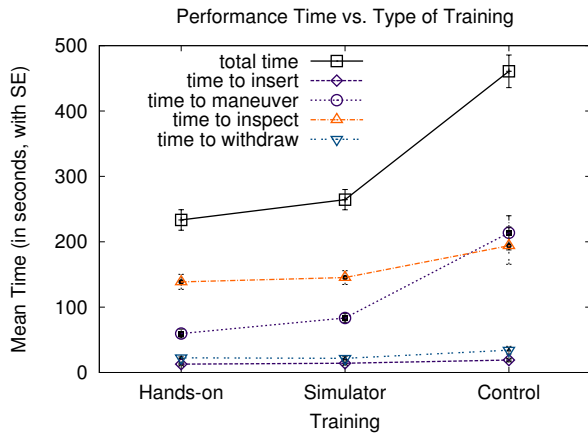


Figure 8: Mean time to insert, maneuver, inspect and withdraw the borescope from the test engine, grouped by type of training provided.

the borescope probe into the engine ($\chi^2(2, N = 26) = 3.06, p > 0.05$), the time taken for inspection of the engine blades for defects ($\chi^2(2, N = 26) = 0.85, p > 0.05$) and withdrawal of the borescope from the engine ($\chi^2(2, N = 26) = 5.18, p > 0.05$). There was a significant difference in the time taken to maneuver the borescope in the engine ($\chi^2(2, N = 26) = 18.61, p < 0.01$), with the control group taking an average of 213 seconds to maneuver the borescope probe through the stators compared to 83 seconds and 59 seconds taken by the simulator and borescope groups, respectively.

Figure 9 shows the mean completion time and the total number of hits of the virtual camera for the simulator training group across day 1 and 2. Repeated measures one-way ANOVA reveals a significant difference in the total time taken for inspection $F(1,8) = 35.09, p < 0.01$. There was no significant difference in the number of hits across the two experiments, $F(1,8) = 0.33, p > 0.05$.

3.6 Discussion

Task completion results across the three groups indicates that participants who received any form of training, either with the virtual simulator or the real borescope, completed the inspection task faster than the control group. The average time taken by the control group was approximately 460 seconds (Figure 8). This is almost double the time taken by participants in other groups with simulator or borescope training. Compared to traditional classroom-only teaching, we find that provision of even limited hands-on training with either the simulator or the real borescope improves inspection performance.

The skill required to perform borescope inspection, especially hand-eye coordination, is difficult to obtain except through hands-on training. As very few aircraft maintenance schools can afford a real borescope, there are limited opportunities for novice students to gain hands-on experience. The similar performance of the simulator and the real borescope groups could be attributed to the similar task profiles and skills needed for inspection. Like the video borescope, the simulator adopted a two handed interaction strategy by using the dominant hand for probe insertion and the non-dominant hand for camera articulation. The indirect manipulation and remote viewing of the component being inspected by the borescope had similar constraints as the virtual simulator.

Although the control group took longer to finish the inspection, a majority of the difference in the time could be attributed to the longer time taken by the participants in maneuvering the borescope through the engine (see Figure 8). Participants in the control group took 2-3 times longer, on average, than those in groups that received

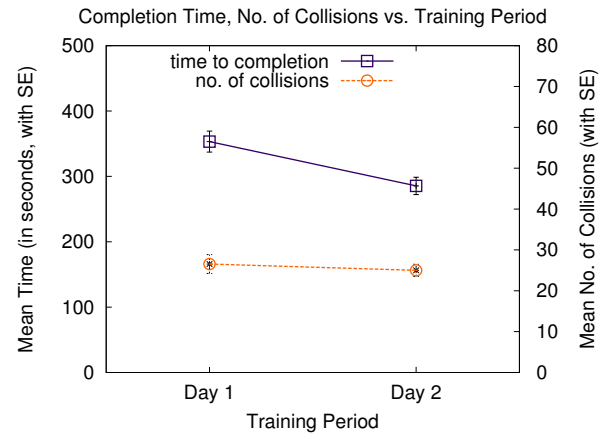


Figure 9: Time taken for simulated inspection and total number of virtual probe collisions evaluated at the end of each training day.

training (213 seconds in control groups versus 59 seconds and 83 seconds for the borescope and simulator training group). Participants with no training were disoriented when using the borescope and had to repeatedly turn their attention away from the video screen to look at the hand-held articulation controls, as well as to balance the borescope probe inserted into the engine. On the other hand, participants with simulator or borescope training were observed to be more comfortable interacting with the controls and with the video screen.

There were no significant differences in the mean time taken by the participants in the three groups for the other stages of the inspection. Probe insertion and withdrawal are similar tasks and lend themselves to easy training in the classroom. The guide tube provides an easy outlet to insert the borescope through the different stages of the engine, and depending on the stage of the engine under inspection, novice inspectors can be instructed to choose the correct guide tube.

The task simulated is representative of borescope inspection performed on an aircraft engine. Once inserted into the engine, the borescope is usually held steady in one place and the rotors being inspected manually rotated. Although defect identification is an important aspect of the simulation, the skills needed for inserting the probe through various stages of the engine are more critical to prevent damage to the probe. The provision of force feedback in the simulator may have helped the participants in transitioning from the simulator to the real world task. This is important as experienced inspectors rely on force feedback from the borescope probe to prevent accidental damage to the probe during insertion and withdrawal from the engine.

Although the number of intersections of the virtual camera with the engine model in the simulator did not significantly decrease during training, provision of tip force feedback may have played a role in transferring skills to the real world. Unlike the simulator, there was no opportunity to collect the total number of intersections of the actual borescope with the engine during inspection. Informal discussions with the participants using the simulator suggested that they preferred the force feedback from the simulator as it aided them in interacting with the simulator, especially while maneuvering the virtual probe into the model.

4 CONCLUSION & FUTURE WORK

The results of this study are significant for two reasons. First, evidence shows that any form of hands-on training is better than classroom-only instruction. Participants were able to relate bet-

ter to inspection procedures through training with either the real borescope or the virtual simulator. Second, and more importantly, results suggest that the skills needed to manipulate the borescope probe that are obtained through on-the-job training may be acquired by novice aircraft maintenance inspectors through simulator training. Similar to pilots gaining flight experience through simulator training, the virtual borescope could be useful in improving student outcomes at aviation maintenance schools. Given the costs associated with obtaining different engines and borescopes for inspection training, virtual simulators integrated with classroom learning may be useful for acquiring sufficient inspection competency for a faster transition to the aviation maintenance workforce.

Simulator training outcomes can be improved in a number of ways. Unlike real inspection, we conducted the evaluation of simulator training by focusing on only the probe manipulation skills needed during the inspection. The engine used for testing the participants was free from defects such as stress cracks, corrosion, and rust. The focus of a future study could be expanded to detect and identify defects (search and decision tasks) by continuing training with the simulator and comparing performance in the workforce.

ACKNOWLEDGEMENTS

We thank the volunteers at Greenville Tech Aircraft Maintenance School for their participation. This work was partially funded by National Science Foundation ATE grant #0703061.

REFERENCES

- [1] T. Alderliesten, M. K. Konings, and W. J. Niessen. Simulation of minimally invasive vascular interventions for training purposes. *Computer Aided Surgery*, 9:3–15, 2004.
- [2] M. W. Allgaier and S. Ness, editors. *Visual and Optical Testing*. Number 8 in Nondestructive Testing Handbook. American Society for Nondestructive Testing, Columbus, OH, 1993.
- [3] L. M. Auer, D. Auer, and J. F. Knoploch. Virtual Endoscopy for Planning and Simulation of Minimally Invasive Neurosurgery. *Lecture Notes in Computer Science*, 1205:315–318, 1997.
- [4] F. Barbagli, D. Prattichizzo, and K. Salisbury. *Multi-point Interaction with Real and Virtual Objects (Springer Tracts in Advanced Robotics)*. Springer-Verlag New York, Inc., Secaucus, NJ, USA, 2005.
- [5] N. Becherer, J. Hesser, U. Kornmesser, D. Schranz, and R. Männer. Interactive physical simulation of catheter motion within major vessel structures and cavities for asd/vsd treatment. volume 6509, page 65090U. SPIE, 2007.
- [6] S. Bobo and C. Puckett. *Visual Inspection for Aircraft, Draft Advisory Circular AC-43-XX*. Federal Aviation Administration, 1995.
- [7] S. N. Bobo. Visual inspection as an organized procedure. *Nondestructive Evaluation of Aging Aircraft, Airports, Aerospace Hardware, and Materials*, 2455(1):164–172, 1995.
- [8] J. Brown, J.-C. Latombe, and K. Montgomery. Real-time knot-tying simulation. *The Visual Computer: International Journal of Computer Graphics*, 20(2):165–179, 2004.
- [9] F. Conti, F. Barbagli, R. Balaniuk, M. Halq, C. Lu, and D. Morris. The CHAI Libraries. In *Eurohaptics '03*, pages 496–500, 2003.
- [10] F. Conti, O. Khatib, and C. Baur. Interactive Rendering Of Deformable Objects based on a Filling Sphere Modeling Approach. In *IEEE International Conference on Robotics and Automation*, volume 3, pages 3716–3721, 2003.
- [11] S. Cotin, C. Duriez, J. Lenoir, P. Neumann, and S. Dawson. New approaches to catheter navigation for interventional radiology simulation. In *Proceedings of medical image computing and computer assisted intervention (MICCAI)*, pages 300–308, 2005.
- [12] S. L. Dawson, S. Cotin, D. Meglan, D. W. Shaffer, and M. A. Ferrell. Designing a computer-based simulator for interventional cardiology training. *Catheterization and Cardiovascular Interventions*, 51(4):522–527, 2000.
- [13] A. Ferlitsch, P. Glauninger, A. Gupper, M. Schillinger, M. Haefner, A. Gangl, and R. Schoefl. Evaluation of a Virtual Endoscopy Simulator for Training of Gastrointestinal Endoscopy. *Endoscopy*, 34(9):698–702, 2002.
- [14] A. Ferlitsch, P. Glauninger, A. Gupper, M. Schillinger, M. Haefner, A. Gangl, and R. Schoefl. Virtual endoscopy simulation for training of gastrointestinal endoscopy. *Endoscopy*, 34(9):698–702, 2002.
- [15] J. A. Ferwerda. Three Varieties of Realism in Computer Graphics. In *Human Vision and Electronic Imaging*, pages 290–297, Bellingham, WA, 2003. SPIE.
- [16] G. M. Fried, L. S. Feldman, M. C. Vassiliou, S. A. Fraser, D. Stanbridge, G. Ghitulescu, and A. C. G. Proving the value of simulation in laparoscopic surgery. *Annals of Surgery*, 240(3):518–528, 2004.
- [17] M. A. Guadagnoli and T. D. Lee. Challenge Point: A Framework for Conceptualizing the Effects of Various Practice Conditions in Motor Learning. *Journal of Motor Behavior*, 36(2):212–224, 2004.
- [18] B. Kubiak, N. Pietroni, F. Ganovelli, and M. Fratarcangeli. A robust method for real-time thread simulation. In *VRST '07: Proceedings of the 2007 ACM symposium on Virtual reality software and technology*, pages 85–88, New York, NY, USA, 2007. ACM.
- [19] P. Lamata, E. J. Gomez, F. Bello, R. L. Kneebone, R. Aggarwal, and F. Lamata. Conceptual framework for laparoscopic vr simulators. *IEEE Computer Graphics and Applications*, 26(6):69–79, 2006.
- [20] S. Laycock and A. Day. Recent developments and applications of haptic devices. *Computer Graphics Forum*, 22(2):117–132, 2003.
- [21] S. D. Laycock and A. M. Day. Incorporating haptic feedback for the simulation of a deformable tool in a rigid scene. *Computers and Graphics*, 29(3):341–351, 2005.
- [22] J. Lenoir, S. Cotin, C. Duriez, and P. Neumann. Interactive physically-based simulation of catheter and guidewire. *Computers and Graphics*, 30(3):416–422, 2006.
- [23] S. Loncaric, T. Markovinovic, T. Petrovic, D. Ramljak, and E. Sorantin. Construction of Virtual Environment for Endoscopy. In *Proceedings of the IEEE International Conference on Multimedia Computing and Systems*, 1999.
- [24] W. Nowinski and C.-K. Chui. Simulation of interventional neuroradiology procedures. *Proceedings of International Workshop on Medical Imaging and Augmented Reality*, pages 87–94, 2001.
- [25] D. K. Pai. Strands: Interactive simulation of thin solids using cosserat models. *Computer Graphics Forum*, 21(3):347–352, 2002.
- [26] D. C. Ruspini, K. Kolarov, and O. Khatib. The haptic display of complex graphical environments. In *SIGGRAPH '97: Proceedings of the 24th annual conference on Computer graphics and interactive techniques*, pages 345–352, New York, NY, USA, 1997. ACM Press/Addison-Wesley Publishing Co.
- [27] G. Saupin, C. Duriez, and S. Cotin. Contact model for haptic medical simulations. 5104:157–165, 2008.
- [28] N. E. Seymour, A. G. Gallagher, S. A. Roman, M. K. O'Brien, V. K. Bansal, D. K. Andersen, and R. M. Satava. Virtual Reality Training Improves Operating Room Performance: Results of a Randomized, Double-Blinded Study. *Annals of Surgery*, 236(4):458–464, 2002.
- [29] D. Vembar, A. T. Duchowski, A. K. Gramopadhye, and C. Washburn. Improving Simulated Borescope Inspection with Constrained Camera Motion and Haptic Feedback. In *Proceedings of Graphics Interface*, 2009.
- [30] F. Wang, E. Burdet, A. Dhanik, T. Poston, and C. L. Teo. Dynamic thread for real-time knot-tying. In *WHC '05: Proceedings of the First Joint Eurohaptics Conference and Symposium on Haptic Interfaces for Virtual Environment and Teleoperator Systems*, pages 507–508, Washington, DC, USA, 2005. IEEE Computer Society.
- [31] F. Wang, L. Duratti, E. Samur, U. Spaelter, and H. Bleuler. A Computer-Based Real-Time Simulation of Interventional Radiology. In *29th Annual International Conference of the IEEE Engineering in Medicine and Biology Society (IEEE-EMBS)*, 2007.
- [32] B. G. Witmer and M. J. Singer. Measuring Presence in Virtual Environments: A Presence Questionnaire. *Presence*, 7(3):225–240, 1998.
- [33] C. Zilles and J. Salisbury. A constraint-based god-object method for haptic display. *Proceedings. 1995 IEEE/RSJ International Conference on Intelligent Robots and Systems 95, 'Human Robot Interaction and Cooperative Robots'*, 3:146–151, Aug 1995.